Chapter

Crystallization and Microstructure of Palm Oil

Fien De Witte, Lennaert Sanders, Koen Dewettinck and Filip Van Bockstaele

Abstract

In addition to being widely available and affordable, its semisolid nature at ambient temperature makes palm oil (PO) a popular ingredient for the food industry. This semisolid nature, consistent with the presence of a fat crystal network that entraps oil, is necessary to create food products that are technologically, sensorially, and nutritionally functional. The crystalline structure of lipids consists of a complex hierarchical structure, ranging from angstroms for polymorphic spacings, over nanometers for chain length structure and crystal nanoplatelet (CNP) sizes, to micrometers for CNP aggregates and flocs. To enable macroscopic lipid functionality, a deep understanding of the distinct structural levels and their interplay is a prerequisite. While X-ray scattering is ideally suited to study the smallest crystalline structures (polymorph, chain length, and CNP), microscopy is necessary to extend the characterization of the fat crystal network toward the microscale. This book chapter provides an overview of the latest insights into the microstructure development of PO using state-of-the-art techniques.

Keywords: microstructure, fat crystallization, hierarchical structure, X-ray scattering, microscopy

1. Introduction

Over the years, palm oil (PO) has become the main lipid source for the production of food products such as frying oils, confectionery products, margarines, and shortenings [1]. Containing equivalent amounts of saturated (myristic, palmitic, and stearic acid) and unsaturated (oleic and linoleic acid) fatty acids (FAs), PO has a competitive advantage over other vegetable oils. Since PO is richer in saturated FAs, it is semisolid at ambient temperature and thus provides structure in several food matrices. The morphology of the solid fraction, presenting itself as a fat crystal network, has significant implications for the technological, sensorial, and nutritional properties of the food products containing it.

Upon cooling the liquid oil, nuclei are formed, and crystal growth proceeds gradually (**Figure 1**). In order to control the macroscopic fat properties, a thorough understanding of the distinct structural levels of the fat crystal network (nanoscale:

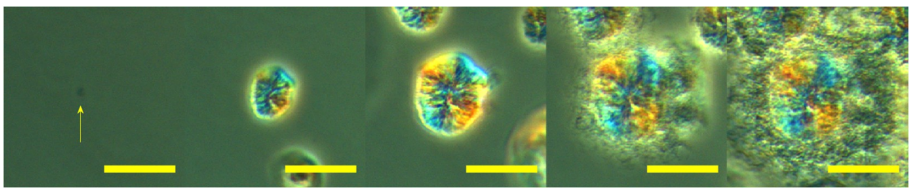

Figure 1.
Polarized light microscopy images showing the growth evolution of a crystal floc when palm oil is crystallized at 25°C. Scale bar 20 μm; the arrow indicates the initial crystal (data from the FSF research group at Ghent University).

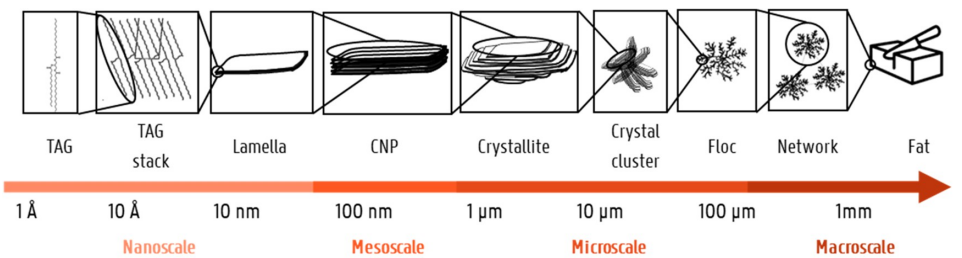

Figure 2.
Multiscale organization of the fat crystal network, reproduced and adapted from Ref. [10].

0.1 nm–100 nm; mesoscale: 100 nm–1 μm; microscale: 1 μm–200 μm; macroscale: >200 μm) is a prerequisite [2]. **Figure 2** illustrates the different hierarchical levels of the fat crystal network.

At the nanoscale, lamellar stacks of triacylglycerols (TAGs) are formed. The polymorphic form of the TAG stacks is of interest. Polymorphism relates to the ability of molecules to arrange themselves in crystal lattices with different subcell packings. For lipids, these different polymorphs are due to the characteristic packing of the hydrocarbon chains of the TAG molecules during fat crystallization [3]. There are three main polymorphic forms for lipids (in increasing order of stability): α, β′, and β [4]. In general, the polymorph formed is related to TAG composition and processing conditions.

During crystallization, TAGs typically adopt the "chair" or "tuning fork" conformation and stack together to form TAG layers or lamellae [3, 5]. These lamellae most commonly adopt a two-chain (2 L) or three-chain (3 L) stacking, although four and six-chain stackings also exist [6]. Lamellae stacked on top of each other form the crystal nanoplatelet (CNP). The CNP owes its name to its platelet-like shape [7]. Some authors tend to use the term "domain," specifically referring to the stacking of lamellae and thus the thickness of the CNP [6].

CNPs arrange themselves into brick-like crystallites, which can be plate-like or needle-like [6, 8, 9]. The crystallites then group themselves into an asterisk-like structure, either fanning out from a central point [9] or more randomly attached at their sides [6], referred to as a "cluster." Several clusters aggregate into flocs, often represented as spherical structures. The flocs can be connected by weak-link interactions, resulting in the formation of a (fractal) network that can entrap oil [8].

Taking into consideration its widespread applications, in the last decades, PO has been a focal point for many researchers and industries. Although each study covers specific aspects of the fat crystal network, the different scales are seldom combined, as this would require a wide analytical toolbox.

2. Nanoscale

PO has a rather simple FA composition, dominated by palmitic acid (P, C16:0, 45.4 ± 0.1%), stearic acid (S, C18:0, 4.4 ± 0.1%), oleic acid (O, C18:1, 38.4 ± 0.1%), and linoleic acid (L, C18:2, 9.4 ± 0.1%). The quantities indicated in parentheses refer to the sample used in the figures of this chapter. Consequently, the TAG composition is focused on higher equivalent carbon numbers (ECNs, as determined via high-pressure liquid chromatography): 3.1% ECN 44, 20.6% ECN 46, 65.6% ECN 48, and 9.8% ECN 50. For example, 2.2% PLL/MOL, 1.9% LOO, 9.9% SLL/PLO, 8.9% PLP/MOP, 5.2% OOO, 24.6% POO, 30.1% PPO/PSL, 5.7% PPP, 3.0% SOO, 5.7% PSO, and 1.1% PPS [11]. Variations in these values exist, and interested readers are referred to Danthine and Gibon [12], who reported ranges of TAG contents based on multiple PO samples sourced from different origins.

Based on its TAG composition, the thermogram of PO consists of two melting and two crystallization fractions, as displayed in **Figure 3**. The high-melting fraction consists mainly of PPP, POP, PPO, and POO, while the low-melting fraction consists of OOO, PLO, and POL. The latter fraction remains liquid at ambient temperature, acting as a solvent for the crystallizing high-melting TAG fraction. The presence of different fractions makes PO ideally suited for fractionation, where a softer (olein) and harder (stearin) fraction are obtained. Although this has been the topic of interest for many researchers, it is beyond the scope of the current chapter, and readers are referred elsewhere [13–16].

At the nanoscale, the polymorphic form (subcell) of the TAGs is imperative for a fat's macroscopic functionality. More specifically, for PO, the polymorphic tendency depends on the content of palmitic acid, the ratio of palmitic to stearic acid, and the distribution of the FAs over the TAGs (monoacid vs. mixed acid) [17–19].

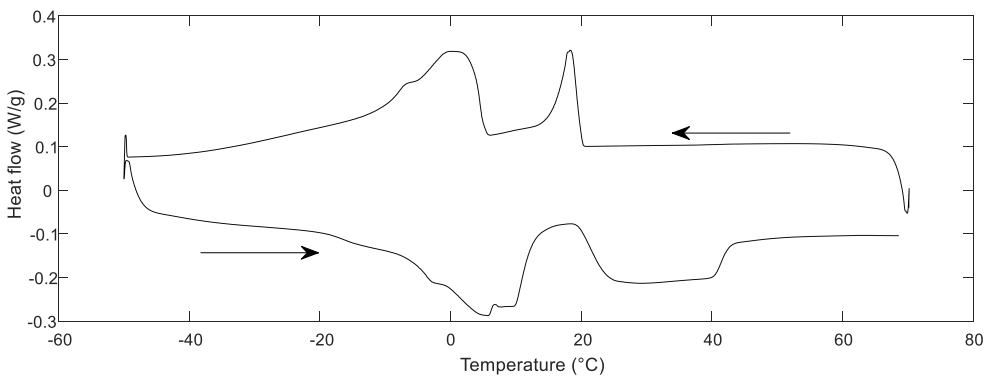

Figure 3.
Differential scanning calorimetry thermogram of palm oil between 70°C and −50°C at a rate of 5°C/min. Arrows indicate the direction of crystallization and subsequent melting (data from the FSF research group at Ghent University).

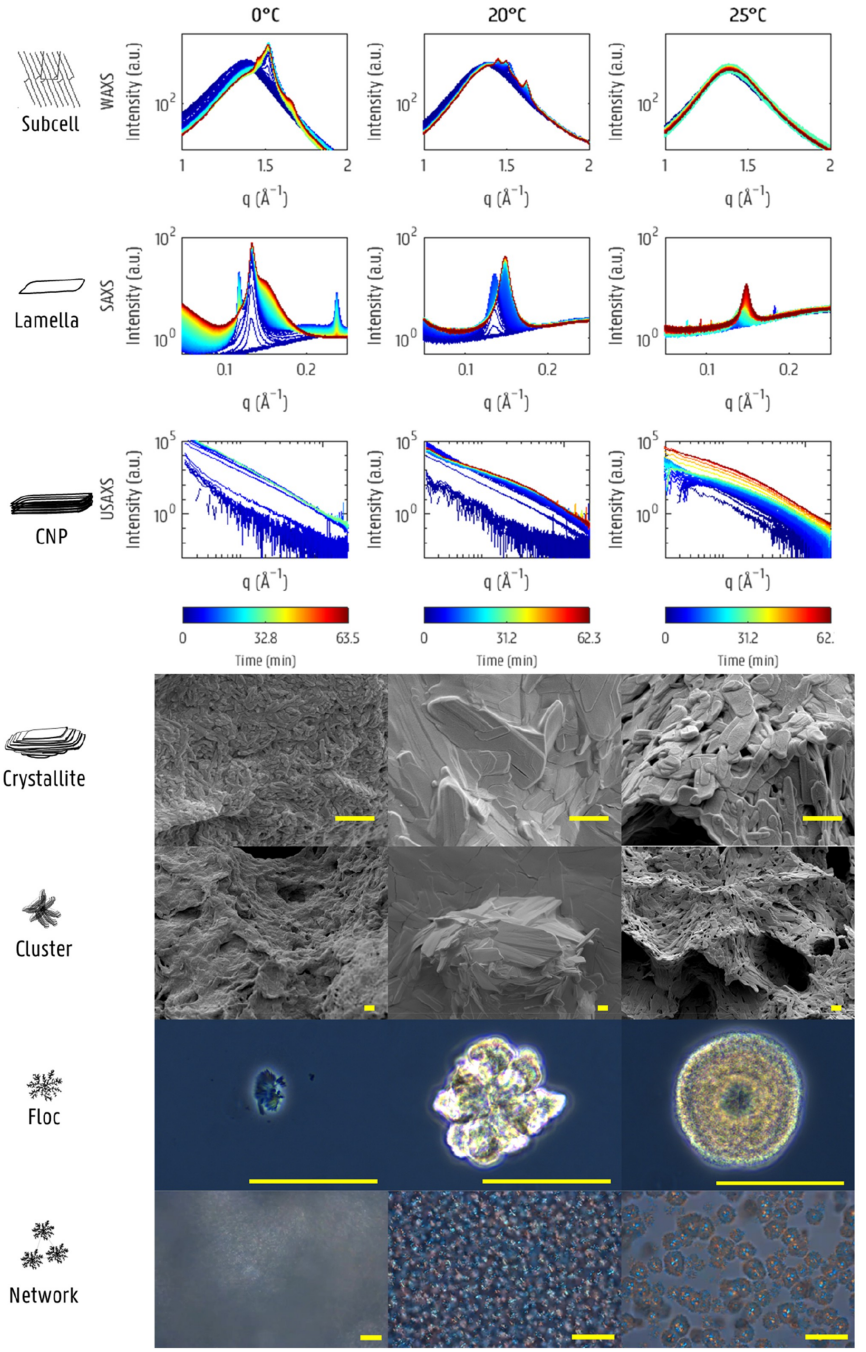

Figure 4.

Overview of palm oil crystallized at 0, 20, or 25°C (left to right) when cooling from 70°C at a rate of 20°C/min. From top to bottom: wide-angle X-ray scattering for subcell identification, small-angle X-ray scattering for chain length structure identification, and ultra-small-angle X-ray scattering for CNP size and shape identification. Cryo-scanning electron microscopy images, magnification 20,000 × (scale bar = 1 μm show crystallites, while magnification 5,000 × (scale bar = 100 μm) illustrates clusters. Phase contrast microscopy illustrates deoiled palm oil flocs (scale bar = 50 μm). Polarized light microscopy was used to visualize fat crystal network (scale bar = 100 μm) (data from FSF research group at Ghent University).

Unlike the β preferential polymorphic tendency of pure tripalmitin (PPP), the preferential polymorphic tendency of PO is β' [7]. For more information on the crystallization of PPP, the reader is directed toward Penagos et al. [10].

X-ray scattering remains the most widely accepted technique for the identification of crystal polymorphs [20]. Each polymorph, along with its corresponding subcell, has been widely characterized, and specific spacings have been attributed to each of the subcells: the α polymorph has a hexagonal subcell, characterized by a short spacing of 4.15 Å; β' has an orthorhombic subcell, with spacings of 3.80 Å and 4.20 Å; and lastly, β has a triclinic subcell with a short spacing of 4.60 Å [21]. The main advantage of X-ray techniques is that samples can be measured in situ. The technique is non-destructive, requires only small amounts of sample, and the results are assumed to be statistically significant as many crystal structures contribute to it [22]. Performing X-ray scattering essentially requires a source of X-rays and a detector. Based on the angles studied, one differentiates between: (1) wide-angle X-ray scattering (WAXS), (2) small-angle X-ray scattering (SAXS), and (3) ultra-small-angle X-ray scattering (USAXS) [22]. De Witte et al. [11] were the first to present time-resolved WAXS-SAXS-USAXS data for PO (**Figure 4**). Their results are briefly discussed below.

WAXS analysis is used to study subcell (polymorph) formation over time. Initially, the WAXS profile consists of a broad feature ($q = 1.36$ Å^{-1}), indicative of the oil present. A slight change in the peak position toward $q = 1.39$ Å^{-1} appears when cooling is applied, which is related to the structuring of the liquid TAGs [23]. At 0°C, 20°C, and 25°C, the α to β' transition was evidenced. The higher the temperature, the shorter the lifetime of the least stable (α) polymorph. It is known that PO is a β'-tending fat due to the presence of asymmetric mixed-acid TAGs, such as POO and PPO, and that this polymorph results in the desired properties for many applications [3]. In addition, based on the WAXS profiles found for 20°C and 25°C, a minority amount of the β polymorph might be present. This polymorph has been reported in PO, for example, at very low cooling rates or after prolonged storage [3, 13].

SAXS is routinely applied to study the chain-length structure of TAGs. Well-ordered TAG crystallites produce a set of scattering peaks at small scattering angles associated with the layered packing of lipid molecules. Lipid-based systems typically produce a strong first-order SAXS peak, alongside weaker higher-order peaks, especially when detecting them with lab-scale instruments. For this reason, the focus is on the shape analysis of the first-order scattering peak [24, 25].

When PO is fast-cooled and crystallized at 0°C, initially, a peak consistent with a 2 L chain length structure ($d = 46.2$ Å) has been found [26]. Some minutes later, an extra peak appeared ($d = 52.4$ Å), which has been described with the term 'ϕ-phase' by Sainlaud et al. [7]. This phase is considered to be a precursor for the triple chain length structure (3 L) and to have limited viability. Over time, the initial α-2 L peak overlaps with the β'-2 L peak ($d = 41.3$ Å). Although both polymorphs form a 2 L lamellar structure, they differ in their angle of tilt, rendering the perpendicular distance of the lamella shorter for β' [27]. Over the time frame of one hour, no indication of the 3 L chain length structure was found. The 2 L form is most common for PO; 3 L is only formed at very specific cooling temperatures [7]. For 20°C, an α-2 L to β'-2 L transition was also observed. The SAXS profile found for 25°C in **Figure 4** was more scattered, and lower overall peak intensities were reached due to the lower

Cooling protocol	SAXS			USAXS		
	d_{001} (Å)	Average # lamella Scherrer (-)	Average # lamella BWA (-)	Slope low q (-)	Cut-off point ($Å^{-1}$)	Slope high q (-)
20°C/min–0°C	Overlapping peaks			Immediate saturation due to high solid-fat content.		
20°C/min–20°C	42.1 ± 0.1	12.0 ± 0.1	10.1 ± 0.1	1.9	0.0051	3.5
20°C/min–25°C	42.1 ± 0.1	12.7 ± 0.2	10.6 ± 0.3	2.2	0.0025	3.4

Table 1.
Parameters obtained from SAXS and USAXS analysis when palm oil was crystallized for one hour using different cooling protocols [11, 28].

amount of fat that crystallizes at 25°C compared to 0°C and 20°C; nonetheless, a similar transition was encountered [11, 28].

3. Mesoscale

The stacking of lamellae results in the formation of CNPs [29]. These CNPs, comprising the mesoscale, are the fundamental building blocks of the lipid hierarchy. The Scherrer equation, based on the full width at half maximum (FWHM) of the first-order diffraction peak, is a commonly used and straightforward method to derive the average domain size and, thus, the average number of lamellae stacked above each other in the CNP (**Table 1**). For PO, an average of 12.0 ± 0.1 and 12.7 ± 0.2 lamellae were found for crystallization at 20°C and 25°C, respectively. As the polymorphic transition at 0°C was incomplete and an overlap of the α-2 L and β'-2 L peaks was present, this sample was not considered in the discussion. The domain size, assumed to be the smallest dimension of the CNP, measured approximately 500 Å [11]. In contrast, Sainlaud et al. [7] showed, by means of the Scherrer formula, that domain sizes increased when applying a slower cooling rate and a lower isothermal temperature (–5, 5, 15, and 25°C).

Alternatively, the Bertaut-Warren-Averbach (BWA) method provides a distribution of the number of lamellae making up the CNPs [25]. After one hour of isothermal crystallization, around 60% of the CNPs consisted of 3–10 lamellae and about 40% of 11–20 lamellae, resulting in domain sizes of 127 to 1,013 Å [11]. As shown in **Table 1**, trends unraveled by the BWA method are similar to those of the Scherrer equation. Nonetheless, the average number of lamellae calculated by the BWA method was lower, which is in line with earlier reports [2, 25].

Fat crystals grow quickly laterally and slowly axially, which results in thin, long, and CNPs [25]. USAXS, an extension of the SAXS technique toward the smallest detectable angles ($2\theta < 0.1°$), can be used to study CNP formation [22]. Contrary to WAXS and SAXS, USAXS data do not consist of distinct peaks. The curves are composed of straight segments and bent sections (**Figure 4**), and their interpretation using models is not straightforward. The Unified Fit model is commonly applied [30–32]. Each fitting level is believed to correspond to a single structural level, approximated as spherical scatterers. One structural level can be described by a

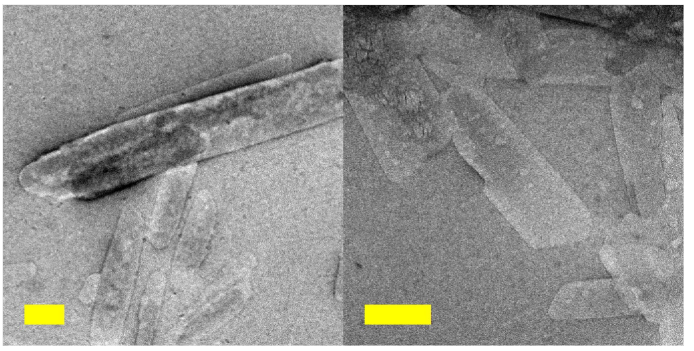

Figure 5.
Transmission electron microscopy image of CNPs of PO, crystallized at 20°C/min to 20°C, scale bar = 200 nm [11].

combination of a power-law or Porod region [33] for the larger q-values and a Guinier region [34] at the smaller q-values. More recently, Penagos et al. [35] developed a new fitting approach in which the CNPs are assumed to be parallelepipeds rather than spheres, based on microscopy insights (**Figure 5**).

The USAXS data shown in **Figure 4** comprise the range of $0.0003\ Å^{-1} < q < 0.02\ Å^{-1}$, implying that information is yielded about structures roughly between 30 nm and 2 μm in size [11]. Considering the structural hierarchy of lipids (**Figure 2**), USAXS enables us to detect CNPs. Before cooling, when the lipids remain liquid, the USAXS profile is dominated by noise (**Figure 4**). Cooling results in an overall increase in USAXS intensity, indicative of a decrease in TAG mobility. Upon reaching the crystallization temperature, the straight profile transforms into an S-shaped curve. Here, the different levels can be seen, where each level (bending section) is joined by two straight lines. These bending sections are indicative of the CNP size. After one hour of isothermal crystallization, the interpretation of the final profile is made by separating the straight zones (one at low q and one at high q) from the bent zone. In order to allow readers to compare the discussed data with their own results, the straight parts of the profiles obtained after one hour of crystallization are characterized by their slope, while the bending zone is defined as the cut-off point, that is, the end of the straight zone at higher q [11].

The interpretation of the USAXS data starts from higher q to lower q (smallest scatterer features first). The straight section at high q is called the Porod region [22]. At this length scale (>30 nm), the electron density contrast comes from the liquid-solid (oil-fat) interface. For 20°C, the decay is found to be P = 3.5, which is close to 4 but deviates, probably because the contrast between liquid and solid fat is not well defined [11]. The bending section appears when the CNPs are formed, and the cut-off point at $q = 0.0051\ Å^{-1}$ is indicative of the average scatterer size. The scatterer shape can be derived from the straight section at lower q. A decay to the power of 1.9 corresponds to a flat, lamellar-based shape [36], as evidenced by the TEM images in **Figure 5**. Taking into account the three different dimensions of a platelet and the polydispersity thereof, it is impossible to give a simple value for its size, but a comparison of the samples is possible [36].

At 25°C, the USAXS profile only shows a weak bend, which can be explained by the low solid fat content (SFC) at this temperature, the low scattering power of the

CNPs, and their expected size polydispersity. The bending section was situated toward lower q (cut-off 0.0025 $Å^{-1}$) compared to at 20°C, which indicates that larger CNPs are formed at 25°C. Furthermore, the profile is characterized by decay to the power of 2.2 at low q, equally indicating platelet-like scatterers. At high q, the curve decays to the order of 3.4, similar to at 20°C (**Table 1**). When crystallizing at 0°C, the USAXS profiles saturated because of the high SFC and the lack of electron density contrast [28]. The USAXS experiment was stopped earlier (**Figure 4**) and we conclude that USAXS is well-suited for studying low solid samples [6, 11, 28, 36, 37].

Gao et al. [38] studied PO diluted at a ratio of 1:3 in soybean oil (SO) at 26°C, with the addition of 1 wt% glycerin monostearate and 1.5 wt% polyglycerol polyricinoleate. The authors used SAXS and applied the Unified Fit equation [39, 40], finding an average CNP diameter of 88.1 nm. Penagos et al. [41] reported, via the parallelepiped model, CNP thicknesses of 26 nm and 25 nm, and widths of 147 nm and 132 nm for 30% PPP and 10% palm stearin samples (15°C), respectively.

4. Microscale

While X-ray scattering is ideally suited to study the smallest crystalline structures (polymorph, chain length structure, and CNP size), microscopy is necessary to visualize hierarchical structures at the meso- and microscale. Recently, several authors have used cryo-scanning electron microscopy (cryo-SEM). This technique is ideally suited to visualize flocs, clusters, crystallites, and even some CNPs, provided that the sample has been deoiled. Researchers have applied different temperatures and used different solvents in this regard: PO with isobutanol [11, 28, 37], PPP with ethanol [6], palm stearin with 80/20% v/v hexane/acetone [10], cocoa butter, milk fat, and palm kernel oil with ethanol [36]. **Figure 4** provides an overview of microscopy images illustrating the meso- and microscale for PO crystallized at 0°C, 20°C, and 25°C. At 0°C, many small CNPs are found. Upon increasing the crystallization temperature, the CNP size increases, and a clear stacking of CNPs into crystallites can be seen. At 25°C, where crystallization is slower, the formation of clusters making up the crystal flocs is equally visible.

Polarized light microscopy (PLM) is the most commonly applied technique to visualize a fat's microstructure. Despite the need for dilute samples, a camera connection can provide real-time crystallization information (**Figure 1**). **Figure 4** illustrates the crystal flocs formed after one hour at 0°C, 20°C, or 25°C.

When cooling to 0°C or 20°C, the driving force for nucleation is high, resulting in multiple small-sized crystal flocs that grow at a high rate [11, 28]. As a result, at 0°C, crystallization is fast, and it is difficult to differentiate between singular flocs. Therefore, in **Figure 4**, the individual flocs are visualized via PLM after deoiling. When cooling rapidly to 25°C, the incentive for nucleation is substantially lower, decreasing the number of nuclei and flocs formed over time. Initially, when crystallization started in the α polymorph (**Figure 4**), dense spherical crystals were formed, as illustrated in **Figure 1**. Later on, concomitantly with the polymorphic transition to the β' polymorph, the flocs grew, showing needle-like crystals pointing outward from the center. As concluded from **Figure 4**, no evidence was found for remaining α crystals after one hour of isothermal crystallization at 25°C.

Only recently, Raman spectroscopy has gained interest in studying the microstructure of fat-based systems [11, 39–42]. In fact, Raman spectroscopy

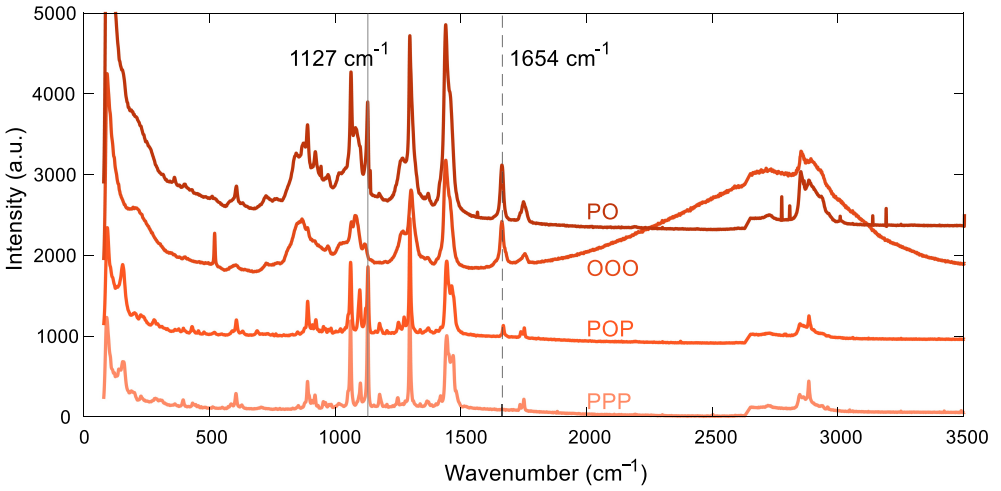

Figure 6.
Raman spectra of references. PO = palm oil, OOO = triolein, POP = dipalmitoyl-oleoyl-glycerol, PPP = tripalmitin. Spectra are vertically shifted for readability (data from FSF research group at Ghent University).

combines chemical and structural characterization of the sample, coupled with spatial information. Lately, advances in Raman microscopy have provided insight into the spatial distribution of triglycerides in PO flocs [11]. To achieve this, Raman spectra of pure TAGs are necessary as references (**Figure 6**). PPP was selected as it is the key driver for the crystallization of the high-melting fraction of PO [43]. From the reference profiles and based on the literature, two characteristic Raman shifts were selected: wavenumber 1,127 cm^{-1} (C–C stretching/C–O–C vibration) was identified as characteristic of the saturated fraction (consisting mainly of PPP), while 1,654 cm^{-1} (C=C stretching) was used to characterize the more unsaturated (and thus liquid) areas of the sample [23, 44].

Figure 7 (left) shows the light microscopy image of a floc formed when PO was crystallized at 25°C. The area selected for Raman mapping measured 45 μm × 50 μm and was mapped by 90 × 100 points, using a 785 nm diode laser. The heatmap shown in **Figure 7** (right) illustrates the ratio of the Raman band at 1,127 cm^{-1} to that at 1,654 cm^{-1}, calculated at every point of the mapping.

The Raman heatmaps clearly distinguished the solid network (high ratio, yellow-white color) from the liquid oil (low ratio, red color). One could differentiate three distinct zones within the sample crystallized at 25°C, based on the TAG profile [11]. Most centrally, a small core presented itself with a band ratio >1.5, showing clear correspondence to the PPP-related band and much less to the OOO-band. This finding corresponds to the floc centers as evidenced in **Figure 1**. The area surrounding the floc center showed medium intensity (ratio 1.0–1.5) for both the PPP- and OOO-band. In addition to the trisaturated PPP, this area probably also contained mono-unsaturated TAGs, such as dipalmitoyl-oleoyl-glycerol (POP). Finally, the outer part of the floc had the lowest PPP-to-OOO-band ratio (<1). Although seen by PLM as a diffuse part of the floc, and thus the crystalline material of the fat, the Raman bands indicate a large presence of unsaturated FAs [11].

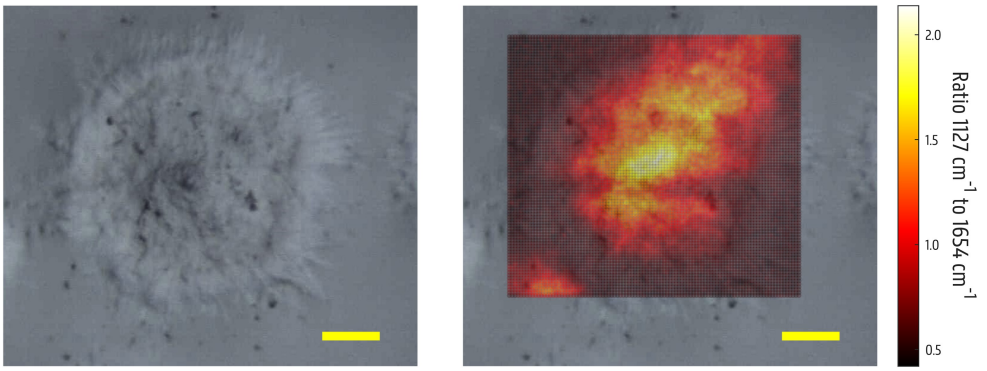

Figure 7.
Light microscopy image of a palm oil floc, crystallized at 25°C (left), and its corresponding Raman spectroscopy mapping (right). Colors refer to the intensity ratio of the band at 1,127 cm^{-1} to that of 1,654 cm^{-1}. Scale bars = 10 μm (data from the FSF research group at Ghent University).

5. Macroscale

While it is meaningful from a fundamental perspective to understand the formation of the fat crystal network from the nano to the microscale, its functionality on the macroscale is of paramount importance to industry. Research by Sanders et al. [37] investigated how the fat crystal network may influence sensorial properties by examining its role in determining rheological and tribological properties at temperatures relevant to oral processing. It was shown that a fraction of high-melting crystalline flocs, suspended in a continuous oil phase, remained present (to a minor extent) at 35°C (**Figure 8**).

Differences in the quantity and morphology of the crystalline fraction impacted the tribological behavior in several lubrication regimes. The authors hypothesized that this occurs either (i) indirectly by affecting the lubricant's bulk (oil phase)

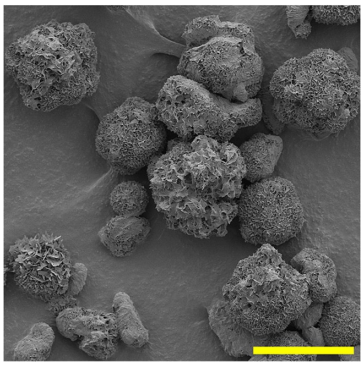

Figure 8.
Cryo-scanning electron microscopy image of crystalline flocs observed at 35°C in a palm/canola oil blend (63 wt% palm oil), following slow, quiescent cooling at an average rate of 0.4°C/min. Scale bar: 50 μm (data from FSF research group at Ghent University).

properties or (ii) directly by being present between the tribological surfaces. The latter scenario is referred to as ball-bearing lubrication, which the authors deemed plausible due to the rounded appearance of the crystalline material (**Figure 8**). In this case, the crystalline flocs limit the contact points between the contacting surfaces and change the type of motion from sliding to rolling, thereby lowering friction [37].

With respect to sensorial quality, a common storage problem in palm-based shortenings or margarines is the formation of large granular crystals. Having a size range of 0.1–3 mm, and thus above the oral detection limit, these crystals negatively impact the product's texture and appearance. As summarized in the review by Nguyen et al. [45], the formation mechanism of granular crystals is not entirely resolved. Results point to a combination of internal and external factors. While PO is kinetically stable and functionalized in food products in the β' polymorph [7], granule formation is often (but not always) linked to the formation of the β polymorph. In fact, the composition and compatibility of the blend determine the extent of post-crystallization, while thermal and mechanical processing enable polymorphism and fat crystal size. Approaches to eliminate the formation of these undesirable fat crystals include the addition of crystal modifiers, as well as modifications in the production process [45].

6. Modifications to the fat crystal network

6.1 Influence of additives

Additives are a broad group of molecules that can affect TAG crystallization, either positively or negatively. In general, three aspects are considered important: 1) the effect of external factors, such as temperature; 2) polymorphic matching; and 3) the chemical structure of the minor component [46, 47]. Very similar chemical structures tend to have a templating effect during nucleation and provide a scaffold for the TAG molecules to crystallize upon. Less similar molecules might delay crystallization through their incorporation, while very different chemical structures tend to block the growth sites of the TAG molecules, thereby hampering fast and structurally pure crystallization [46]. Most studies focus on addressing melting behavior, crystallization kinetics, SFC, and microstructure.

A first category of additives is the "minor lipid components," a group of compounds that includes phospholipids, mono and diacylglycerols (MAGs and DAGs), waxes, phytosterols, and free FAs. These components can be naturally present in fats [48], but they can also be deliberately added. For example, native PO can contain up to 4–8% diacylglycerols, which might inhibit nucleation and cause resistance toward the formation of the β' polymorph, resulting in slow crystallization rates [49–52].

Verstringe et al. [53] demonstrated, by means of SR-μ-XRD, the templating effect of monopalmitin. When previously crystallized monopalmitin was added to PO, the crystals were shown to be oriented. However, during storage, PO and monopalmitin crystals separated. Zhang et al. [54] proposed PBP and PSP as effective crystal modifiers, as they enhance nucleation, promote β' formation, and delay the β' to β transformation. Both TAGs have different polymorphic tendencies, with β-3 L for PBP and β'-2 L for PSP. In contrast, BBB enhanced β formation but decreased crystal

size by promoting nucleation [47]. The effects of the crystal modifiers are more limited at higher degrees of undercooling [47, 54].

Chikhoune et al. [55] studied the addition (5 wt%) of essential oils (a mixture of terpenes) from an Algerian plant, which are used for their anti-oxidative properties. The oil addition slowed down the PO crystallization, as evidenced by a lower SFC over time. Effects on the microstructure varied with the composition of the oil.

Cooney et al. [56] investigated the effect of cannabidiol (CBD, 1 or 2.5 wt%) on the crystallization of PO at 26°C. The authors found no effect on the melting point or microstructure, but CBD delayed crystallization as its ring structures are structurally too different from TAGs and hence block the TAG growth sites. The effect was limited in PO but more pronounced in shorter-chain FA sources. Contrary to other fats, the addition of CBD had implications for the physical behavior, rendering the PO samples harder and more elastic.

Another category of additives is dispersing agents. In this category, the use of sucrose esters (SEs), whose FA moieties can be tailored, is popular [28, 57–60].

In our most recent study, the impact of 0.5 wt% of a palmitic-stearic SE on the hierarchical structures of the PO crystal network was investigated [28]. DSC analysis indicated a seeding effect, as the onset of crystallization occurred sooner upon the addition of the SE. The different fractions crystallized over a shorter period of time, and polymorphic transitions occurred earlier. Looking at the nanoscale with WAXS and SAXS, the α-2 L–to-β'-2 L transitions happened earlier and were completed sooner upon the addition of the SE. The Scherrer and BWA analyses, which yield information about the mesoscale, revealed that when using a high cooling rate, the added SE decreased the CNP thickness. The application of USAXS unraveled that CNPs containing SE are smaller than PO CNPs, which was confirmed using cryo-SEM. **Figure 9** (PLM and cryo-SEM images) shows that the addition of the SE resulted in a fine and dense microstructure, implying the co-crystallization of PO and SE [28].

Containing FA chains, it is generally assumed that SEs interact with the fat crystal network via an acyl-acyl interaction. This mechanism implies that SEs with a similar acyl chain length to their surrounding matrix operate as crystal templates to strengthen crystallization, resulting in a homogeneous fat crystal network composed of numerous small entities. Mostly, SEs with unsaturated FA have little effect.

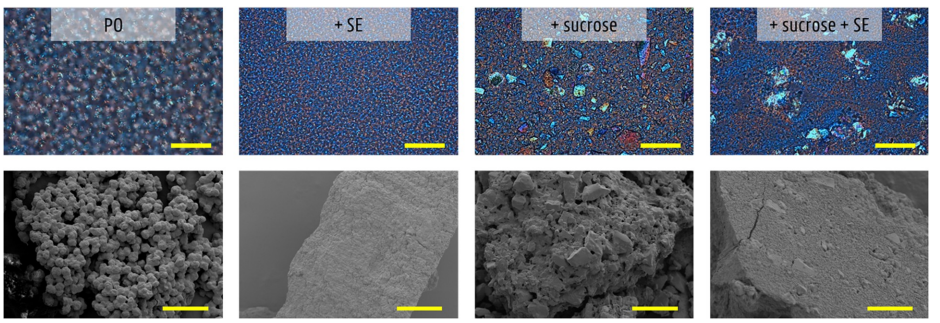

Figure 9.
Polarized light microscopy images (upper) and cryo-scanning electron microscopy images (lower) showing the effect of sucrose addition (10 wt%) and a stearic-palmitic sucrose ester (0.5 wt%) on palm oil crystallized at 20°C. Scale bar = 100 μm (data from FSF research group at Ghent University).

Dissimilarity in the FA chain length, on the other hand, tends to result in delayed crystallization and the formation of large crystals [57, 58, 61]. Additionally, Liu and Binks (2021) [62] discuss the presence of intermolecular and/or intramolecular hydrogen bonds among unsubstituted OH-groups and ester carbonyl groups. Furthermore, the large di-saccharide head group might block crystal growth sites [57, 58, 61].

6.2 Influence of particles

Given the wide variety of confectionery products on the market, research investigating suspensions, that is, dispersions of solid particles in a continuous lipid phase, is essential. Particles provide surfaces at which lipids can nucleate heterogeneously [63]. In addition, the dispersed phase induces changes in the mobility of the TAGs, affecting crystal growth [64]. The impact of dispersed solids on fat nucleation and crystal growth has been studied in chocolate model systems [65–67], real chocolate [42, 43, 63, 64, 68, 69] and sucrose/palm fat dispersions [70, 71].

The effect of sucrose addition to PO was found to depend on the particle size distribution of sucrose [72]. The smallest sucrose particles act as connections between coarser sucrose particles and bulk lipids, thereby reinforcing the network. Research also indicated that the effect can mainly be attributed to the smallest particles. A small portion of sucrose "dust" particles seemed to modify the PO network to a similar extent as PPP addition, which offers a cost-effective solution for modifying fat crystal networks in confectionery systems [72].

De Witte et al. [42] studied PO-based suspensions with sucrose and inulin addition (10 wt%) and combined particle and SE SP30 addition (0.5 wt%). It was found that all additions affected the onset of crystallization, the time of polymorphic transition, and the melting curve. Polymorphic pathways and long spacings were not affected. No differences between sucrose and inulin were found, which aligns with their carbohydrate-nature and similar particle size distribution. The addition of SE combined with the particles was, in general, the most efficient. On the mesoscale, a 10 wt% particle addition was found to slightly decrease the CNP thickness. The USAXS study of the PO-sucrose mixtures revealed that CNP size decreased the most with sucrose and SE (0.5 wt%) addition, and less with sucrose alone. Cryo-SEM analysis showed a significant decrease in CNP size for all suspensions. The study of the microscale with PLM was found to be complex when particles were present, even at a low concentration of 10 wt%. The addition of particles and SE together, in combination with crystallization at 20°C, removed the visibility of separate flocs, while under other conditions (25°C or particle addition alone), small flocs were observed (**Figure 9**). Cryo-SEM and Raman spectroscopy analysis were able to overcome this issue. Particle addition severely decreased the floc size. The results clearly illustrate that particles with a size on the order of micrometers affect scales of a similar size. Similarly, the SE molecules, which are smaller in size, also manage to affect the nanoscale. Similar findings were obtained for inulin compared to sucrose, indicating that there is no effect of the solid state (crystalline vs. glassy) or particle shape [42].

The visualization of the microscale becomes significantly obscured at high levels of dispersed phase, especially when using conventional microscopy techniques [64]. To address this limitation, our laboratory has recently developed a novel method

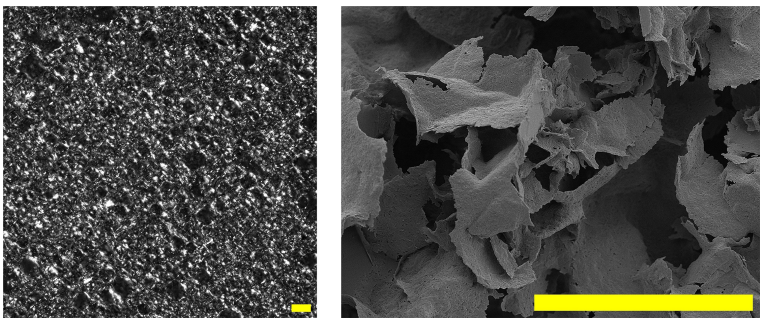

Figure 10.
Microscale illustration of the effect of sucrose addition (40 wt%) to a palm/canola oil blend (63 wt% PO) crystallized at 20°C/min from 70 to 10°C Left: light microscopy image (grayscale), right: corresponding cryo-scanning electron microscopy image. Scale bar = 25 μm (data from FSF research group at Ghent University).

involving the removal of sucrose from fat-continuous suspensions prior to imaging. This approach facilitates the observation of structural features such as crystallites, crystal clusters, and, in certain cases, flocs. Preliminary results are presented in **Figure 10**.

The effects of non-food particles have been equally investigated with the purpose of studying specific particle sizes and specific surface properties. Yoshikawa et al. [73] demonstrated the applicability of 1 wt% inorganic and organic materials as templates for fat crystallization in three types of pure TAGs (LaLaLa, MMM, or PPP). Inorganic particles also promoted fat crystallization and transformation toward the most stable polymorph, although their interaction with the TAGs is not based on hydrophobic interactions, as is the case for organic particles. With respect to particle size and concentration, it was concluded that each of the explored particle sizes (0.6–14 μm) promoted crystallization, even at the lowest particle concentration (0.01 wt%). A decrease from 14 to 2.5 μm ensured additional promotion, while using lower particle sizes delivered no further benefit. Rendering the talc particle more hydrophobic did not change the effects, which leads to the conclusion that for heterogeneous nucleation, the presence of the particle is important, but not its chemical similarity to the fat [74].

Continuing with the talc particles, the authors addressed their effect on a PO-based shortening. It was concluded that the addition of talc enhanced the formation of lower-melting crystals while reducing the amount of higher-melting crystals [75].

Following up on the surface properties, West and Rousseau [43] studied the effect of silica particles with hydrophilic and hydrophobic surface properties on the crystallization of PO under static and sheared conditions. Both silica types were found to enhance nucleation and increase the total enthalpy of melting. Higher concentrations and the hydrophobic silica type were more effective.

6.3 Crystallization under shear

Research on the effect of shear on fat crystallization is highly relevant to the food industry, for example, in the production of margarines and shortenings [48, 76]. In fact, Tavernier et al. [77] demonstrated that the macroscopic properties of statically crystallized lipid systems are not predictive of those produced by a

scraped surface heat exchanger. Studies combining shear and compositional variations concluded that the application of shear results in a reduction of composition-related effects, indicating greater effects of processing compared to composition [43, 78].

Shear affects the different structural development stages of crystallizing fats, such as nucleation, crystal growth, inter-particulate collisions, and polymorphic transitions [79, 80]. Shear often enhances mixed crystal formation and increases the number of smaller crystals, inducing a mechanically stronger crystal network [81], and it promotes β' crystal formation [78]. However, whether shear has a positive impact on the microstructural development of crystallizing fats seems to depend on the level of the applied shear, that is, whether it is below or above a critical shear rate [24, 82]. Shear experiments on a lab scale are often performed on a rheometer equipped with plate-plate or impeller geometry. A shear profile can be imposed on the sample while the viscosity profile is monitored. After the shear step, the crystal network development can be monitored non-destructively by dynamic oscillation rheology as a function of time [83]. Another possibility is to use a plate-plate shear system (Linkam CSS450). This system, originally developed for microscopy purposes, can be modified into an X-ray-proof system, allowing the study of polymorphic pathways over time.

From a recent study by our research group [84], using a CSS450 (gap 1,500 μm), it can be concluded that shear influenced different hierarchical structures of the fat crystal network, from the polymorphism to the microscale. PO was cooled at 20°C/min to 20°C or 25°C, while a shear rate of 1 s^{-1} or 50 s^{-1} was applied during the cooling. Shear was found to enhance nucleation at 20°C, independent of the shear rate. At 25°C, a faster shear rate was more beneficial, and the onset time of crystallization was approximately halved. Additionally, either a low or high shear rate directed the crystallization at 25°C to start from the more stable β' polymorph. On the mesoscale, cryo-SEM images showed that the application of a slow shear rate seemed to elongate the CNPs formed. Furthermore, it was found, by means of cryo-SEM, that shear decreased the floc size and condensed the overall microstructure; however, the effect was similar for both studied shear rates and inferior to the effect of temperature.

7. Conclusion(s)

Over the years, the crystallization of PO has been a field of interest for many researchers. The relevance of PO remains high, considering its widespread applications. Tailoring PO crystallization through various additions or processing methods is a never-ending quest. With ever-improving methodologies becoming available, such as USAXS, more detailed insights are being gained into the structural hierarchy of the palm fat crystal network. Lastly, it can be concluded from this chapter that a multiscale approach is necessary in crystallization studies, as different hierarchical levels might not react in a similar fashion when exposed to changing conditions.

With respect to modifications of the crystal network of palm fat, efforts have been made to separate the effects of internal factors (PO composition, particle addition, dispersing agent, etc.) and external factors (temperature, shear, sonication etc.). It was demonstrated that some factors affect crystallization across the entire

length scale (e.g., temperature and dispersing agent), while others primarily influence the micro- and macroscale (e.g., particles). Even though the effects on crystallization at most hierarchical structures are limited, this does not rule out impacts at the macroscale, including effects on sensory properties, rheology, hardness, and SFC. Research correlating the dynamics of macroscopic properties to smaller-scale insights remains limited.

Acknowledgments

The data presented by the authors were obtained during projects 1128923N and G085021N funded by the Flanders Research Fund (FWO). The FWO is also acknowledged for funding AUGE/09/29 (Hercules grant for cryo-SEM equipment) and AUGE/17/29 (Hercules grant for XRS equipment). We acknowledge the European Synchrotron Radiation Facility (ESRF) for the provision of synchrotron radiation facilities ID02 (ME-1606) and BM26 (A26-2-943). We thank Vandemoortele Lipids NV for providing the samples, as well as their financial support to the Vandemoortele Centre "Lipid Science and Technology."

Conflict of interest

The authors declare no conflicts of interest.

Author details

Fien De Witte*, Lennaert Sanders, Koen Dewettinck and Filip Van Bockstaele
Food Structure & Function Research Group, Ghent University, Ghent, Belgium

*Address all correspondence to: fien.dewitte@ugent.be

References

[1] Aini IN, Miskandar MS. Utilization of palm oil and palm products in shortenings and margarines. European Journal of Lipid Science and Technology. 2007;**109**(4):422–432

[2] Rondou K, et al. Multiscale analysis of monoglyceride oleogels during storage. Journal of the American Oil Chemists' Society 2022;**99**:1019–1031

[3] Marangoni A, Wesdorp LH. Structure and Properties of Fat Crystal Networks. Boca Raton, Florida, USA: CRC Press; 2012

[4] Cholakova D, Denkov N. Polymorphic phase transitions in triglycerides and their mixtures studied by SAXS/WAXS techniques. In: Bulk and in Emulsions. Advances in Colloid and Interface Science. Vol. **323**. Amsterdam, NL: Elsevier; 2024. p. 103071

[5] Himawan C, Starov VM, Stapley AGF. Thermodynamic and kinetic aspects of fat crystallization. Advances in Colloid and Interface Science. 2006;**122**(1):3–33

[6] Mishra K, et al. Controlling lipid crystallization across multiple length scales by directed shear flow. Journal of Colloid and Interface Science. 2023;**630**:731–741

[7] Sainlaud C, et al. Impact of cooling profile on refined palm oil crystallization: Microscopic and small and wide-angle X-ray scattering investigations. European Journal of Lipid Science and Technology. 2022;**124**(2):2100045

[8] Nikolaeva T, et al. Networks of micronized fat crystals grown under static conditions. Food & Function. 2018;**9**:2102–2111

[9] Tang D, Marangoni AG. Quantitative study on the microstructure of colloidal fat crystal networks and fractal dimensions. Advances in Colloid and Interface Science. 2006;**128-130**:257–265

[10] Penagos IA, et al. Unravelling the hierarchical structure of saturated monoacid triglycerides during crystallization – A comprehensive time-resolved X-ray scattering study. CrystEngComm 2024;**26**:6143–6154

[11] De Witte F, et al. Insights in the structural hierarchy of statically crystallized palm oil. Crystals 2024;**14**:142

[12] Danthine S, Gibon V. Comparative analysis of triacylglycerol composition, melting properties and polymorphic behavior of palm oil and fractions. European Journal of Lipid Science and Technology. 2007;**109**:359–372

[13] Gibon V. 10 - Fractionation of lipids for use in food. In: Gunstone FD, editor. Modifying Lipids for Use in Food. Cambridge, UK: Woodhead Publishing; 2006. pp. 201–233

[14] Tong S-C, Tang T-K, Lee -Y-Y. A review on the fundamentals of palm oil fractionation: Processing conditions and seeding agents. European Journal of Lipid Science and Technology. 2021;**123**(12):2100132

[15] Cremer G, Danthine S, Blecker C, and Gibon V. Peculiar crystallisation behaviour of palm oil during dry fractionation. Journal of Oil Palm Research. 2022;**35**(2):296-306

[16] Hishamuddin E, Nagy Z, Stapley A. Thermodynamic analysis of the isothermal fractionation of palm oil using a novel method for entrainment correction. Journal of Food Engineering. 2020;**273**:109806

[17] Bayés-García L, et al. Heterogeneous microstructures of spherulites of lipid mixtures characterized with synchrotron radiation microbeam X-ray diffraction. CrystEngComm 2011;**13**:6694–6705

[18] Macias-Rodriguez B, Marangoni AG. Rheological characterization of triglyceride shortenings. Rheologica Acta. 2016;**55**(9):767–779

[19] Bayés-García L, et al. Crystallization and transformation of polymorphic forms of trioleoyl glycerol and 1,2-dioleoyl-3-rac-linoleoyl glycerol. The Journal of Physical Chemistry B 2013;**117**:9170–9181

[20] Ladd Parada M, et al. Early stages of fat crystallisation evaluated by low-field NMR and small-angle X-ray scattering. Magnetic Resonance in Chemistry. 2019;**57**:686–694

[21] Kalnin D, et al. Fat crystallization in emulsion: Influence of emulsifier concentration on triacylglycerol crystal growth and polymorphism. Crystal Growth & Design. 2004;**4**(6):1283-1293

[22] Peyronel F, Pink DA. Chapter 9 - Ultra-small angle X-ray scattering: A technique to study soft materials. In: Marangoni AG, editor. Structure-Function Analysis of Edible Fats. *Second Edition* ed. Urbana, Illinois, USA: AOCS Press; 2018. p. 267–285

[23] Czamara K, et al. Raman spectroscopy of lipids: A review. Journal of Raman Spectroscopy 2015;**46**:4–20

[24] Acevedo N, Marangoni A. Functionalization of non-interesterified mixtures of fully hydrogenated fats using shear processing. Food & Bioprocess Technology. 2014;**7**(2): 575–587

[25] den Adel R, et al. Fat crystallite thickness distribution based on SAXD peak shape analysis. European Journal of Lipid Science and Technology. 2018;**120**(9):1800222

[26] Bayés-García L, et al. Lipid crystallization kinetics — Roles of external factors influencing functionality of end products. Current Opinion in Food Science. 2015;**4**:32–38

[27] Sato K. Crystallization behaviour of fats and lipids — A review. Chemical Engineering Science. 2001;**56**(7): 2255–2265

[28] De Witte F, et al. From nucleation to fat crystal network: Effects of stearic–palmitic sucrose ester on static crystallization of palm oil. Foods. 2024;**13**:1372

[29] Acevedo NC, Peyronel F, Marangoni AG. Nanoscale structure intercrystalline interactions in fat crystal networks. Current Opinion in Colloid and Interface Science. 2011;**16** (5):374–383

[30] Beaucage G. Approximations leading to a unified exponential/ power-law approach to small-angle

scattering. Journal of Applied Crystallography. 1995;**28**(6): 717–728

[31] Beaucage G. Small-angle scattering from polymeric mass fractals of arbitrary mass-fractal dimension. Journal of Applied Crystallography. 1996;**29**(2): 134–146

[32] Ilavsky J, Jemian P. Irena: Tool suite for modeling and analysis of small angle scattering. Journal of Applied Crystallography. 2009;**42**: 347–353

[33] Porod G. Die röntgenkleinwinke lstreuung von dichtgepackten kolloiden systemen. II. Teil. Kolloid-Zeitschrift. 1952;**125**(2):108–122

[34] Guinier A, Fournet G. Small-angle Scattering of X-rays. Hoboken, New Jersey, USA: Wiley; 1955

[35] Penagos IA, et al. Multiscale analysis of triglycerides using X-ray scattering: Implementing a shape-dependent model for CNP characterization. Soft Matter 2024;**20**:5071–5085

[36] Mishra K, et al. The rheology and foamability of crystal-melt suspensions composed of triacylglycerols. Soft Matter 2022;**18**:1183–1193

[37] Sanders L, et al. Lubricative properties of semi-crystalline lipid systems. Food Structure. 2025;**44**: 100435

[38] Gao Y, Mao J, Meng Z.Network structure and nanoplatelet characterization of the edible fat crystallization in low-fat W/O emulsions. Langmuir. 2023;**39**(26): 8963–8973

[39] Milc KW, et al. Quantifying cooperative flow of fat crystal dispersions. Soft Matter 2022;**18**: 2782–2789

[40] Martens KJA, et al. Quantitative structural analysis of fat crystal networks by means of Raman confocal imaging. Journal of the American Oil Chemists' Society. 2018;**95**:259–265

[41] Penagos IA, et al. Investigating the role of CNP and CNP aggregates in the rheological breakdown of triglyceride systems. Crystals 2024;**14**:566

[42] De Witte F, et al. The effect of particles on static crystallisation in suspensions: Sucrose vs. inulin, in npj science of food (accepted). *Critical Reviews in Food Science and Nutrition*. 2025

[43] West R, Rousseau D.Tripalmitin-driven crystallization of palm oil: The role of shear and dispersed particles. Journal of the American Oil Chemists' Society. 2020;**97**(9):989–999

[44] Glatter O. Chapter 6 - contrast variation. In: Glatter O, editor. Scattering Methods and Their Application in Colloid and Interface Science. Amsterdam: Elsevier; 2018. p. 111–121

[45] Nguyen V, et al. Granular crystals in palm oil based shortening/margarine: A review. Crystal Growth and Design. 2020;**20**:1363–1372

[46] da Silva TLT, Martini S. Recent advances in lipid crystallization in the food industry. Annual Review of Food Science and Technology. 2024;**15** (1):355–379

[47] Zhang L, et al. Monobehenin and tribehenin as modifiers in the

crystallization of palm oil and palm stearin. European Journal of Lipid Science and Technology. 2022;**124** (5):2100220

[48] Patel AR, Dewettinck K. Current update on the influence of minor lipid components, shear and presence of interfaces on fat crystallization. Current Opinion in Food Science. 2015;**3**:65–70

[49] Jacobsberg B, Ho OC. Studies in palm oil crystallization. Journal of the American Oil Chemists' Society. 1976;**53** (10):609–617

[50] Siew W-L, Ng W-L. Influence of diglycerides on crystallisation of palm oil. Journal of the Science of Food & Agriculture. 1999;**79**(5):722–726

[51] Ribeiro AP, et al. Crystallization modifiers in lipid systems. Journal of Food Science and Technology 2015;**52**:3925–3946

[52] Xie P, et al. Potential of diacylglycerol to replace nature fats in conventional plastic fats: Preparation, purification, functionalities and applications. Trends in Food Science and Technology. 2025;**161**:105057

[53] Verstringe S, et al. Triacylglycerol crystal growth: Templating effects of partial glycerols studied with synchrotron radiation microbeam X-ray diffraction. Crystal Growth and Design. 2014;**14**:5219–5226

[54] Zhang Q, et al. PBP and PSP promote β' form crystallization of palm oil, palm stearin, and a cocoa butter replacer. European Journal of Lipid Science and Technology. 2023;**125** (12):2300040

[55] Chikhoune A, et al. Isothermal crystallization of palm oil-based fats with and without the addition of essential oils. Journal of the American Oil Chemists' Society. 2020;**97**(8):861–878

[56] Cooney J, et al. Crystallization behavior of milk fat, palm oil, palm kernel oil, and cocoa butter with and without the addition of cannabidiol. Journal of the American Oil Chemists' Society 2023;**100**:225–236

[57] Garbolino C, Bartoccini M, Flöter E. The influence of emulsifiers on the crystallisation behaviour of a palm oil-based blend. European Journal of Lipid Science and Technology. 2005;**107** (9):616–626

[58] Chen C, et al. Effects of sucrose esters on isothermal crystallization of palm oil-based blend. Journal of the American Oil Chemists' Society 2015;**92**:277–286

[59] Tangsanthatkun J, Sonwai S. Crystallisation of palm olein under the influence of sucrose esters. International Journal of Food Science and Technology. 2019;**54**(11):3032–3041

[60] Domingues MAF, et al. Tailoring crystallization and physical properties of palm mid-fraction with sorbitan tristearate and sucrose stearate. Food Chemistry. 2022;**369**:130943

[61] Rincón-Cardona JA, et al. In Situ Synchrotron Radiation X-ray Scattering Study on the Effect of a Stearic Sucrose Ester on Polymorphic Behavior of a New Sunflower Oil Variety. Vol. **64**. Amsterdam, NL: Food Research International; 2014. p. 9–17

[62] Liu Y, Binks BP. A novel strategy to fabricate stable oil foams with sucrose ester surfactant. Journal of Colloid and Interface Science. 2021;**594**:204–216

[63] West R, Rousseau D. The role of nonfat ingredients on confectionery fat crystallization. Critical Reviews in Food Science and Nutrition. 2018;**58**(11): 1917–1936

[64] West R, Rousseau D. Crystallization and rheology of palm oil in the presence of sugar. Food Research International. 2016;**85**:224–234

[65] Fernandes VA, Müller AJ, Sandoval AJ. Thermal, structural and rheological characteristics of dark chocolate with different compositions. Journal of Food Engineering. 2013;**116**(1):97–108

[66] Sonwai S, Mackley MR. The effect of shear on the crystallization of cocoa butter. Journal of the American Oil Chemists' Society. 2006;**83**(7): 583–596

[67] Szydłowska-Czerniak A, Rabiej D, Pawłowicz R. Comparison of the crystallization behaviors of different types of cocoa butters and chocolates. Journal of Food Processing and Preservation. 2017;**41**(5):e13154

[68] West R, Rousseau D. Modelling sugar, processing, and storage effects on palm oil crystallization and rheology. LWT - Food Science & Technology. 2017;**83**:201–212

[69] West R, Rousseau D. Regression modelling of the impact of confectioner's sugar and temperature on palm oil crystallization and rheology. Food Chemistry. 2019;**274**:194–201

[70] Dhonsi D, Stapley A. The effect of shear rate, temperature, sugar and emulsifier on the tempering of cocoa butter. Journal of FOOD Engineering - J FOOD ENG. 2005; **77**(4):936-942

[71] Svanberg L, et al. Effect of sugar, cocoa particles and lecithin on cocoa butter crystallisation in seeded and non-seeded chocolate model systems. Journal of Food Engineering 2011;**104**:70–80

[72] Hubbes -S-S, Braun A, Foerst P. Sugar particles and their role in crystallization kinetics and structural properties in fats used for nougat creme production. Journal of Food Engineering. 2020;**287**:110130

[73] Yoshikawa S, Kida H, Sato K. Promotional effects of new types of additives on fat crystallization. Journal of Oleo Science. 2014;**63**(4):333–345

[74] Yoshikawa S, Kida H, Sato K. Fat crystallization with talc particles is influenced by particle size, concentration, and cooling rate. European Journal of Lipid Science and Technology. 2015;**117** (6):858–868

[75] Yoshikawa S, et al. Adding talc particles improves physical properties of palm oil-based shortening. European Journal of Lipid Science and Technology. 2016;**118**:1007–1017

[76] De Graef V, et al. Development of a rheological method to characterize palm oil crystallizing under shear. European Journal of Lipid Science and Technology. 2008;**110**:521–529

[77] Tavernier I, et al. Effect of high cooling and shear rate on the microstructural development of hybrid systems containing diacylglycerols and triacylglycerols of palm origin. Journal of Food Engineering. 2019;**246**:141–152

[78] Smith P, et al. Polymorphic and microstructural behaviors of palm oil/ lecithin blends crystallized under shear.

Journal of the American Oil Chemists Society 2022;**99**:665–674

[79] Sato K, et al. External factors affecting polymorphic crystallization of lipids. European Journal of Lipid Science and Technology. 2013;**115**(11):1224–1238

[80] Tran T, Rousseau D. Influence of shear on fat crystallization. Food Research International. 2016;**81**:157–162

[81] Campos R, Marangoni A. Crystallization dynamics of shear worked cocoa butter. Crystal Growth and Design. 2014;**14**:1199–1210

[82] Acevedo NC, Block JM, Marangoni AG. Critical laminar shear-temperature effects on the nano- and mesoscale structure of a model fat and its relationship to oil binding and rheological properties. Faraday Discussions. 2012;**158**(0):171–194

[83] De Graef V. Microstructural Properties of Isothermal Palm Oil Crystallization. Ghent University; 2009

[84] De Witte F. Multiscale Assessment of Fat Crystal Networks in Suspensions. Ghent University; 2024